Available online at www.sciencedirect.com
SCIENCE DIRECT®
Journal of Pharmaceutical and Biomedical Analysis
35 (2004) 9–19
JOURNAL OF PHARMACEUTICAL AND BIOMEDICAL ANALYSIS
www.elsevier.com/locate/jpba

The photocatalytic process as a tool to identify metabolitic products formed from dopant substances: the case of buspirone

Paola Calza, Marco Pazzi, Claudio Medana*, Claudio Baiocchi, Ezio Pelizzetti

Dipartimento di Chimica Analitica, Università di Torino, via P. Giuria 5, 10125 Torino, Italy

Received 8 September 2003; received in revised form 23 December 2003; accepted 3 January 2004

Abstract

The photocatalytic transformation of buspirone, an analgesic anxiolytic drug, and the formation of intermediates products have been evaluated by adopting titanium dioxide as a photocatalyst. Several molecules resulting from buspirone degradation have been identified and characterized by using HPLC/MS/MS technique. The main intermediates formed in these experimental conditions agree with the major buspirone metabolites found "in vivo" on rats and horses: hydroxy and dihydroxy-buspirone, despyrimidinyl buspirone and 1-pyrimidinyl piperazine. This shows that the photocatalytic system could provide in the present case a useful simulation of the metabolic transformation of dopant substances. Moreover, some more oxidized species have been recognized with the photocatalytic process, and this could offer a suggestion for yet to come metabolism studies.

Keywords: Buspirone; Metabolites; Doping control; Photocatalysis

1. Introduction

The purpose of this study is to utilize the photocatalytic process to artificially produce metabolitic products reasonably similar to those really present in the metabolic system of living organisms. This methodological approach has already been successfully used in the case of dexamethasone [1].

As a target molecule we have chosen buspirone, an analgesic drug widely used in anxiolytic therapy [2–5] which is largely lacking in sedative or muscle-relaxant side-effects [6,7]. This substance is also illegally used as dopant on horses by contributing to calm high-spirited horses, so improving their performance during the race.

The identification of possible metabolic structures may be very useful in order to search also these species in the animal after the race. Several metabolic studies on buspirone are already available [8–12]; in vivo metabolic studies have been performed on rats [11] and horses [12]. The more suitable technique of analysis to identify and characterize the main transformation products coming from buspirone is represented by the HPLC coupled with a mass spectrometer [13–16]. In the present study will be presented a comparison between the intermediates found by adopting a

* Corresponding author. Tel.: +39-011-6707636; fax: +39-011-6707615.
E-mail address: claudio.medana@unito.it (C. Medana).

0731-7085/$ – see front matter © 2004 Elsevier B.V. All rights reserved.
doi:10.1016/j.jpba.2004.01.001

photocatalytic process (using titanium dioxide as a photocatalyst) and those found into in vivo experiments on rats and horses.

2. Experimental section

2.1. Material and reagents

All experiments were carried out using TiO_2 Degussa P25 as the photocatalyst. In order to avoid possible interference from ions adsorbed on the photocatalyst, the TiO_2 powder was irradiated and washed with distilled water until no signal due to chloride, sulfate or sodium ions could be detected by ion chromatography.

Buspirone (Aldrich) was used as received. HPLC grade water was obtained from MilliQ System Academic (Waters Millipore). Methanol HPLC grade (BDH) was filtered through a 0.45 μm filter before use. Ammonium acetate reagent grade was purchased from Fluka Chemie.

2.2. Irradiation procedures

The irradiations have been performed using a 1500 W xenon lamp (Solarbox, CO.FO.MEGRA, Milan, Italy) simulating AM1 solar light and equipped with a 340 nm cut-off filter. The total photons flux (340–400 nm) in the cell and the temperature during irradiation has been kept constant for all experiments. They were 1.35×10^{-5} einstein min^{-1} and 50 °C, respectively. The irradiation was carried out on 5 ml of suspension containing 15 mg l^{-1} buspirone and 200 mg l^{-1} TiO_2. The entire content of the cells was filtered through a 0.45 μm filter and then analyzed by an HPLC-MS instrument.

2.3. Analytical procedures

2.3.1. Liquid chromatography

The chromatographic separations were run on a C18 column Merck Lichrospher, 250 mm × 4.6 mm (Merck). Injection volume was 80 μl and flow rate 0.8 ml min^{-1}. Gradient mobile phase composition was adopted: methanol/aqueous ammonium acetate 20 mM, pH 3.3, 10:90 to 100:0 in 45 min.

2.3.2. Mass spectrometry

A LCQ MAT ion trap mass spectrometer (ThermoFinnigan) equipped with an atmospheric pressure interface and an ESI ion source was used. The LC column effluent was delivered into the ion source using nitrogen as sheath and auxiliary gas (Claind Nitrogen Generator apparatus). The spray voltage was set at the 4.5 kV value. The acquisition method used was previously optimized in the tuning sections for the parent compound (capillary, magnetic lenses and collimating octapoles voltages) in order to achieve the maximum of sensitivity. The tuning parameters adopted for ESI source have been the following: capillary voltage 3.00 V, heated capillary temperature 220 °C, tube lens 0 V; for ions optics, multipole 1 offset –5.00 V, electrostatic lens voltage −34.00 V, multipole 2 offset –7.50.

3. Results and discussion

3.1. Buspirone

3.1.1. Photocatalytic transformation

The disappearance of buspirone as a function of the irradiation time is reported in Fig. 1, showing a pseudo-first order kinetic and the achievement of the complete abatment of the primary compound until 30 min. Being the principles and mechanism of photocatalysis on TiO_2 surface well-known and widely documented [17–20], here it will be only briefly

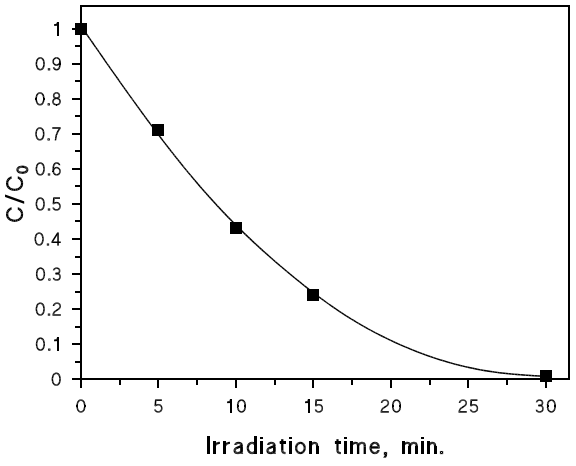

Fig. 1. Disappearance of buspirone (15 mg l^{-1}) on TiO_2 Degussa P25 200 mg l^{-1} as a function of irradiation time.

introduced the main reactions. When irradiating with photons of energy equal to or exceeding the band gap energy of titanium dioxide (anatase, 3.2 eV band gap), valence band (VB) electrons are promoted to the conduction band (CB). Valence band holes [$E_0 = +3.1$ eV versus NHE at pH 0] and reductive conduction band electrons ($E_0 = -0.1$ eV) are generated:

$$TiO_2 + h\nu \rightarrow e^-_{CB} + h^+_{VB} \quad (1)$$

The photogenerated electrons and holes can recombine giving a null process or they can migrate to the surface of the particle before recombination occurs. The photodecomposition of buspirone could thus be carried out either by oxidative species or conduction band electrons. In particular, the oxidizing species may be holes (h^+_{VB}, more oxidizing than the aqueous hydroxy radical) or trapped holes (less oxidizing than the aqueous hydroxy radical) [21]. The photogenerated holes can directly oxidize the adsorbed buspirone or producing adsorbed OH radicals [22,23] through the surface bound OH^- or the adsorbed H_2O molecules.

The reducing species may be conductive band electrons or trapped electrons, both less reducing than aquated electrons [19,24]. The photogenerated electrons could reduce the buspirone or react with the adsorbed molecular oxygen with superoxide radical anion $O_2^{\bullet -}$ formation.

3.1.2. MS/MS study

Buspirone has been characterized through a MS^2 study. Confirmation of the molecular weight can be obtained by the MS spectrum which exhibited $[M+H]^+$ 386 ion as base peak (see Table 1), while MS^2 could be applied using *m*/*z* 386 as precursor ion. The

Table 1
Main fragments coming from MS^2 of the species represented in Scheme 8

$[M+H]^+$	Proposed structure	No.	Retention time (min)	MS^2 fragments
386	Buspirone	I	15.41	122(100), 222(60), 186(40), 150(28), 265(26), 180(8), 291(4)
402	Hydroxy-buspirone	II[a,b]	14.54	384(100), 138(10), 222(9), 166(8), 265(7), 291(4), 402(10)
	Hydroxy-buspirone	III[a]	10.76	122(70), 150(45), 238(100), 402(15), 178(5), 219(50), 281(15), 307(4)
	Hydroxy-buspirone	IV[a]	10.06	122(100), 150(30), 238(45), 195(59), 402(28), 281(25), 307(10), 359(5), 385(10)
	Hydroxy-buspirone	V[a]	11.30	122(23), 150(40), 238(100), 178(3), 402(3), 307(4), 281(5), 219(63)
418	Dihydroxy-buspirone	VI[a,b]	11.26	344(100), 138(3), 166(3), 225(6), 281(3), 238(5), 358(15), 373(8), 400(15), 307(2)
	Dihydroxy-buspirone	VII[a,b]	10.13	138(5), 166(5), 220(4), 238(6), 281(3), 307(3), 400(100)
165	1-Pyrimidinyl piperazine	VIII[a]	4.93	122(100), 165(2)
308	Despyrimidinyl buspirone	IX[a]	9.45	308(20), 222(10), 180(9), 152(11), 168(12)
350	Despyrimidinyl buspirone-amidine	X	8.99	112(2), 222(4), 265(6), 291(100), 308(55), 333(10), 180(2)
366	Despyrimidinyl-hydroxy-buspirone-amidine	XI	4.76	
	Despyrimidinyl-hydroxy-buspirone-amidine	XII	8.0	308(100), 222(40), 180(9)
400	Oxo-buspirone	XIII	10.20	122(100), 150(26), 236(24), 279(28), 305(5), 357(5), 400(8)
	Oxo-buspirone	XIV	11.68	122(100), 150(33), 194(24), 236(40), 279(30), 305(5), 357(7), 400(20)

The relative abundances are reported in parentheses.
[a] Metabolites found in rats [11].
[b] Metabolites found in horses [12].

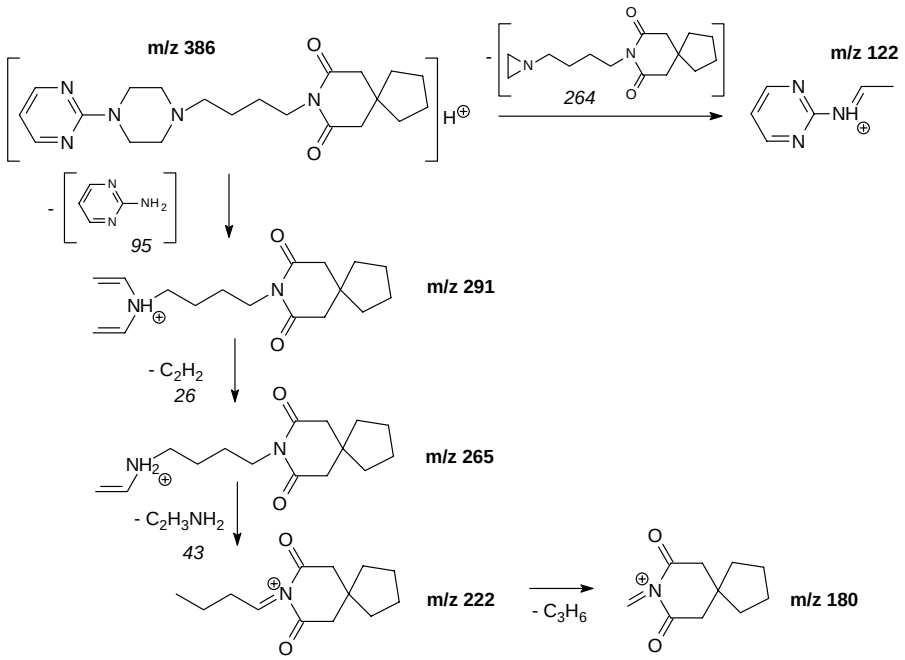

Scheme 1. Fragmentation pathway followed by buspirone.

peculiar information extractable from the MS/MS spectrum are reported in Table 1. The main fragments can be linked through the fragmentation pathway is shown in Scheme 1.

These fragments will be carefully considered in identifying the metabolic structures formed from buspirone degradation. In particular, the product ion at *m*/*z* 122 will be indicative of the unchanged pyrimidine substructure, while the *m*/*z* 222 and 180 ions are diagnostic of the unchanged azaspirone decane dione substructure.

3.2. Intermediates evolution

Concomitantly to the disappearance of buspirone, the formation of several peaks characterized by different *m*/*z* ratios is realized. Fig. 2 shows the obtained chromatographic profile of the solution at 10 min of degradation as an example. As it can be observed, numerous species have been identified, characterized by different *m*/*z* ratios along with several peaks corresponding to an equal *m*/*z* value.

The kinetics of formation and decomposition followed by the intermediates need also to be determined in order to individuate the more stable compounds. The evolution of the different peaks as a function of the irradiation time is reported in Figs. 3 and 4, where typical bell shaped profiles of intermediates are shown. On the basis of their chromatographic behavior and kinetics of evolution coupled with an accurate analysis of the MS and MS^2 spectra, the structures reported in Table 1 are suggested. Several of these species have been also discovered into in vivo metabolic studies [11,12]. These structures are collected in Fig. 3 and they have been marked in Table 1 with letter a if have been found in rats [11] or with letter b if they have been found in horses [12]. Some more species have been identified only by adopting the photocatalytic process and they are reported in Fig. 4. A pattern of reactions accounting for the observed species is proposed in Scheme 8.

3.2.1. Structures found both with in vivo study and by a photocatalytic process

3.2.1.1. Hydroxy-buspirone. Several species holding $[M+H]^+$ 402 have been detected (see Figs. 2 and 3) and they are attributed to hydroxy-buspirone (see structures II–V in Table 1). The peculiar fragments observed in the MS/MS spectra for these four species could lead to two different fragmentation pathways,

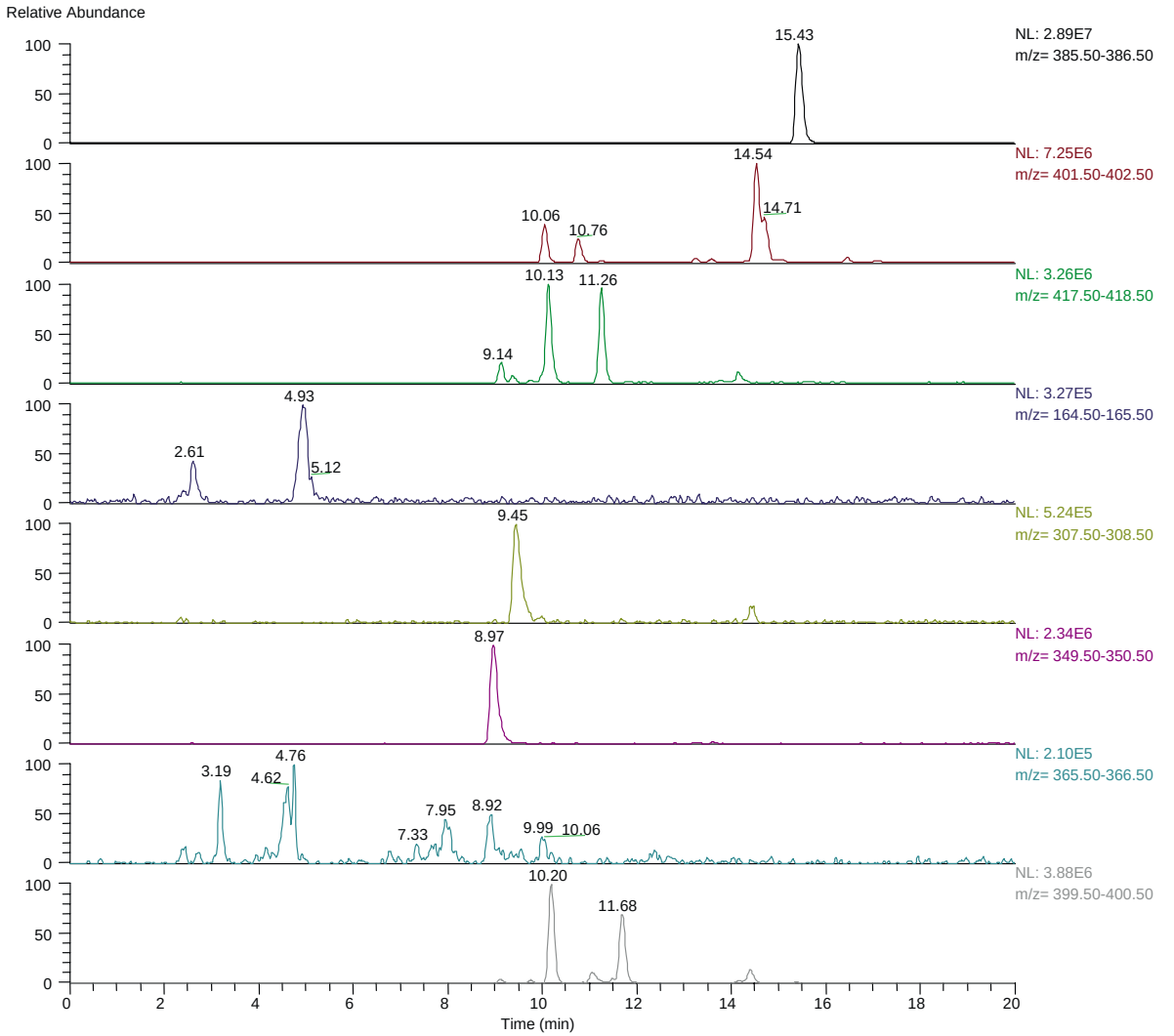

Fig. 2. Chromatographic profile of the solution at 10 min of degradation showing the species formed from the buspirone degradation; ions extracted from full scan chromatogram.

as reported in Scheme 2a and b, so bringing to the identification of structures holding the OH group attack in different positions.

The major hydroxylated metabolite (labeled II in Table 1 and Scheme 8) follows the fragmentation pathway shown in Scheme 2a. Several fragments indicate that the position of hydroxylation is located in the pyrimidine substructure. In particular, the presence of the *m*/*z* 222 ion evidences the intact butyl azaspirone decane dione substructure. The absence of the *m*/*z* 122, together with the appearance of a fragment with *m*/*z* 138 ion, confirms the localization of the hydroxyl group on the pyrimidine substructure.

Three species, labeled III–V in Table 1, present fragments linked by the fragmentation pathway reported in Scheme 2b. The presence of the *m*/*z* 122 ion indicates a metabolite structure containing an intact pyrimidine substructure. Shift of the *m*/*z* 291 to 307 ion, the *m*/*z* 265 to 281 and the *m*/*z* 222 to 238 provides a complementary evidence for hydroxyl substitution on the azaspirone decane dione substructure.

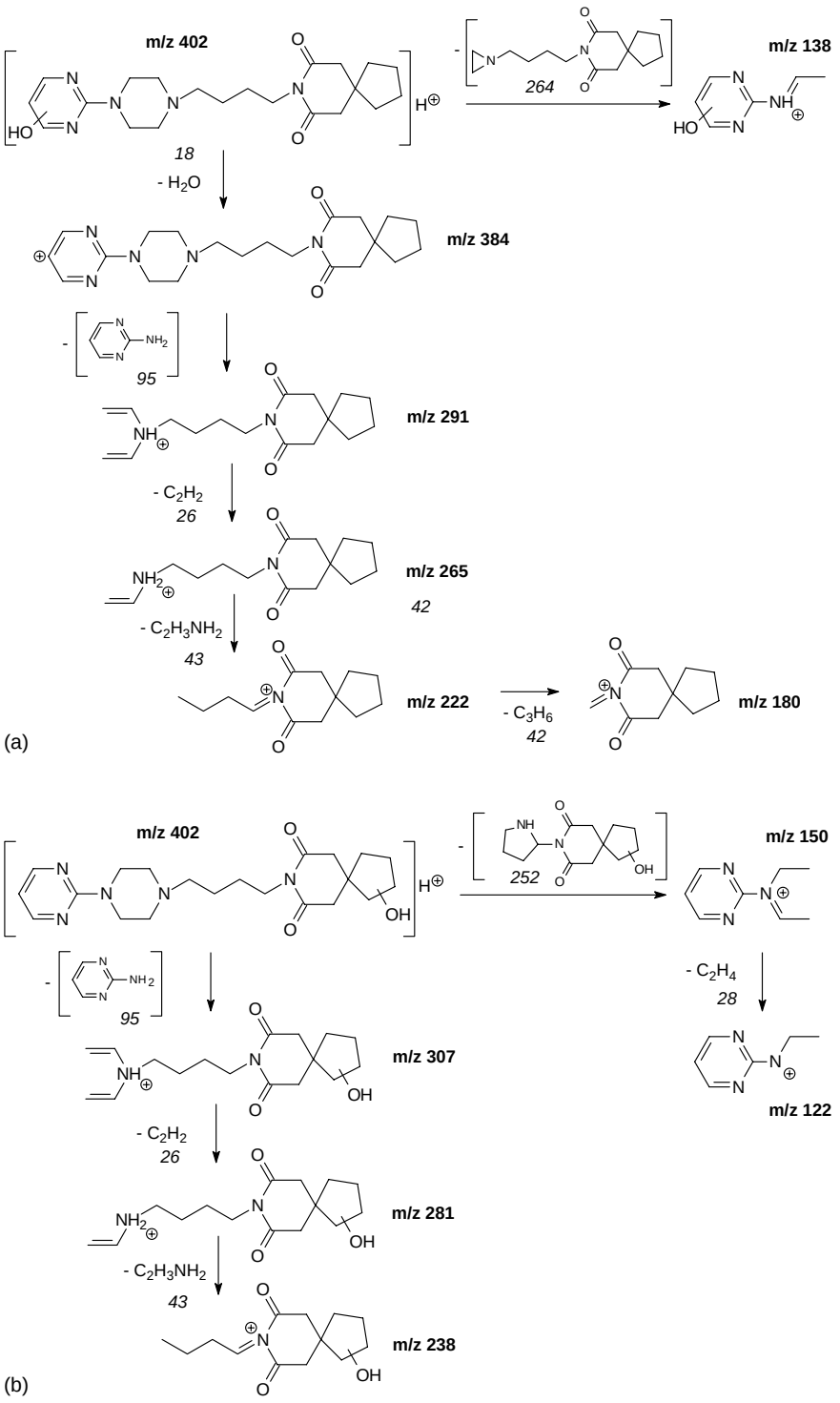

Scheme 2. (a) Fragmentation followed by hydroxy-buspirone (II). (b) Fragmentation followed by hydroxy-buspirone (III–V).

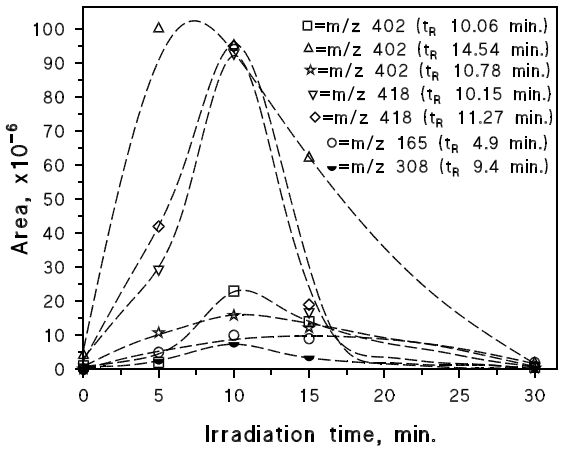

Fig. 3. Evolution of intermediates formed from the disappearance of buspirone (15 mg l^{-1}) degradation on TiO_2 200 mg l^{-1} as a function of irradiation time; structures found also into in vivo experiments.

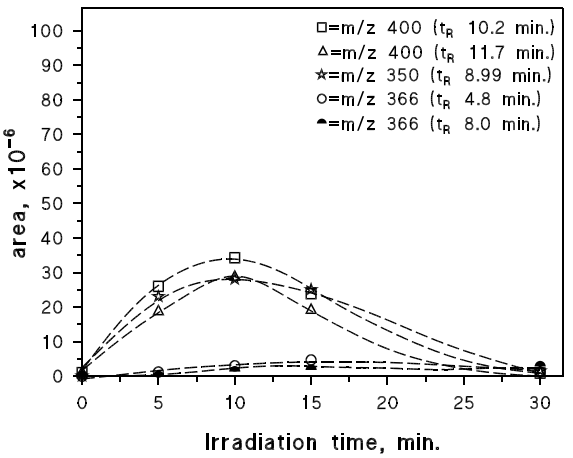

Fig. 4. Evolution of intermediates formed from the disappearance of buspirone (15 mg l^{-1}) degradation on TiO_2 200 mg l^{-1} as a function of irradiation time; structures found only in the photocatalytic process.

Two of these structures are formed in appreciable amount and their kinetic profile are shown in Fig. 3, while the third one (with retention time of 11.30 min) is present only in traces.

3.2.1.2. Dihydroxy-buspirone. Similarly to what observed with the hydroxy-buspirone, two peaks holding the same *m*/*z* ratio (418) have been detected (see Fig. 2). The difference of 32 amu with respect

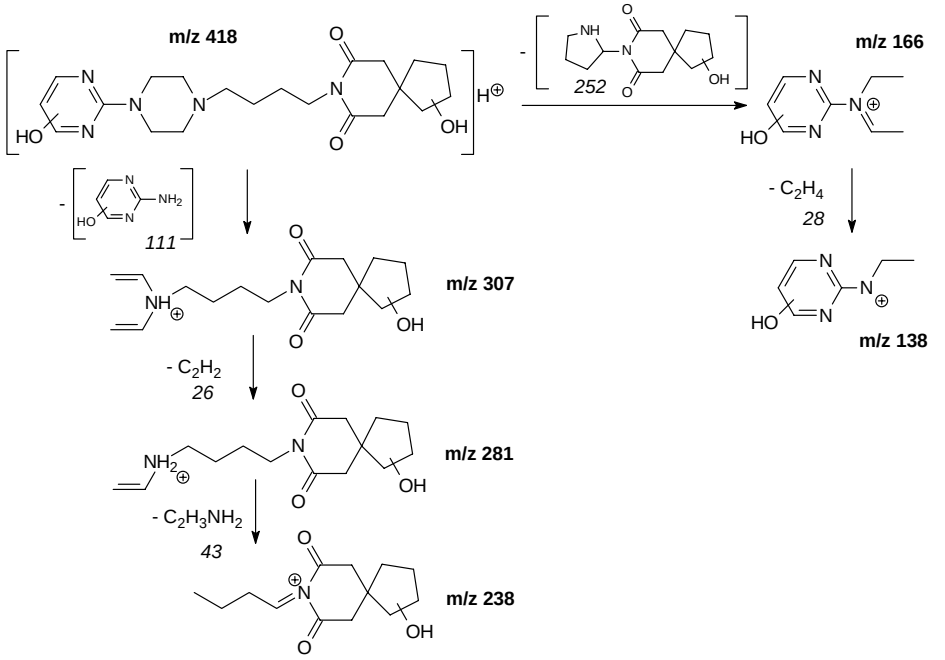

Scheme 3. Fragmentation followed by dihydroxy-buspirone.

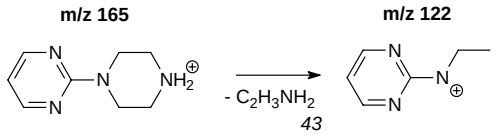

Scheme 4. Fragmentation followed by 1-pyrimidinyl piperazine.

to the parent molecule numerically corresponds to a double OH substitution and they are assigned to the dihydroxy-buspirone (see structures VI and VII in Table 1).

These molecules follow the fragmentation pathway reported in Scheme 3. The absence of the *m*/*z* 122 and 222 indicates that both the pyrimidine and butyl azaspirone decane dione substructures present a substitution. The MS^2 of the parent ion of $[M+H]^+$ 418 shows the presence of the OH-substituted pyrimidine substructure (*m*/*z* 138 and 166) and the product ions at *m*/*z* 238 and 281, which is consistent with the introduction of a second hydroxyl at the butyl azaspirone decane dione substructure. Both species are formed in appreciable amount (see Fig. 3).

3.2.1.3. Despyrimidinyl buspirone and 1-pyrimidinyl piperazine. In addition to the hydroxy and dihydroxy derivatives, two other metabolites have been identified, in which a portion of the buspirone is cleaved off to form 1-pyrimidinyl piperazine (see structure VIII in Table 1) and despyrimidinyl buspirone (see structure IX in Table 1). In both cases, the hypothized structures are supported by the MS/MS spectra. The structure $[M+H]^+$ 165 shows a 221 amu difference compared to the buspirone structure, so in agreement with a loss of the butyl azaspirone decane dione.

In the case of 1-pyrimidinyl piperazine confirmation comes from the absence of all the significative fragments observed for azaspirone decane dione substructure. The only significant fragment has *m*/*z* 122 and comes from the fragmentation of piperazine substructure (see Scheme 4).

For the structure holding $[M+H]^+$ 308, the 78 amu difference from buspirone indicates the loss of pyrimidine. Moreover, in the case of despyrimidinyl buspirone evidence for the absence of the pyrimidine substructure comes from the absence of the *m*/*z* 122 ion, while the presence of the *m*/*z* 222 and 180 ions indicates the intact butyl azaspirone decane dione substructure and the occurrence of the fragmentation pathway is shown in Scheme 5.

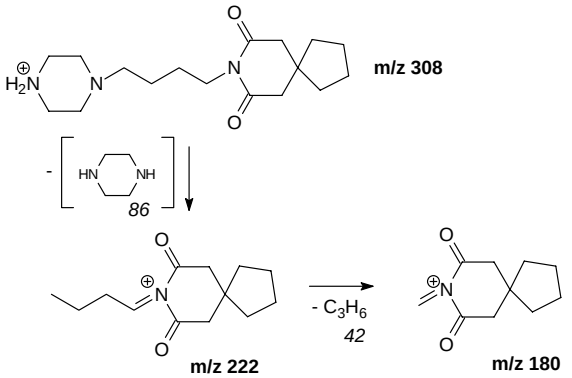

Scheme 5. Fragmentation followed by despyrimidinyl buspirone.

3.2.2. Structures only found by adopting the photocatalytic process

In addition to the species presented above, which have been found with in vivo metabolic experiments, few more species have been only identified (see Fig. 2) by adopting a photocatalytic process and their kinetical profiles are represented in Fig. 4.

3.2.2.1. Structure with $[M+H]^+$ 350. In correspondence to the $[M+H]^+$ 350, only one peak is observed (see structure X in Table 1). This structure represents an intermediate step between the buspirone and the despyrimidinyl buspirone. The fragments observed are linked through the fragmentation pathway indicated in Scheme 6. Analogously to what observed in the case of despyrimidinyl buspirone, the absence of the *m*/*z* 122 ion gives a confirmation of the absence of the pyrimidine substructure, while the presence of the fragments holding *m*/*z* 222 and 181 gives an evidence about the persistence of the unmodified butyl azaspirone decane dione substructure.

3.2.2.2. Structure with $[M+H]^+$ 366. Similarly to what observed for $[M+H]^+$ 350 ion, also this structure has lost the pyrimidine substructure. The 16 amu difference in respect to 350 indicates the presence of an OH group in the butyl azaspirone decane dione substructure. Two peaks have been observed at the same *m*/*z* (see Fig. 2). These structures probably come from

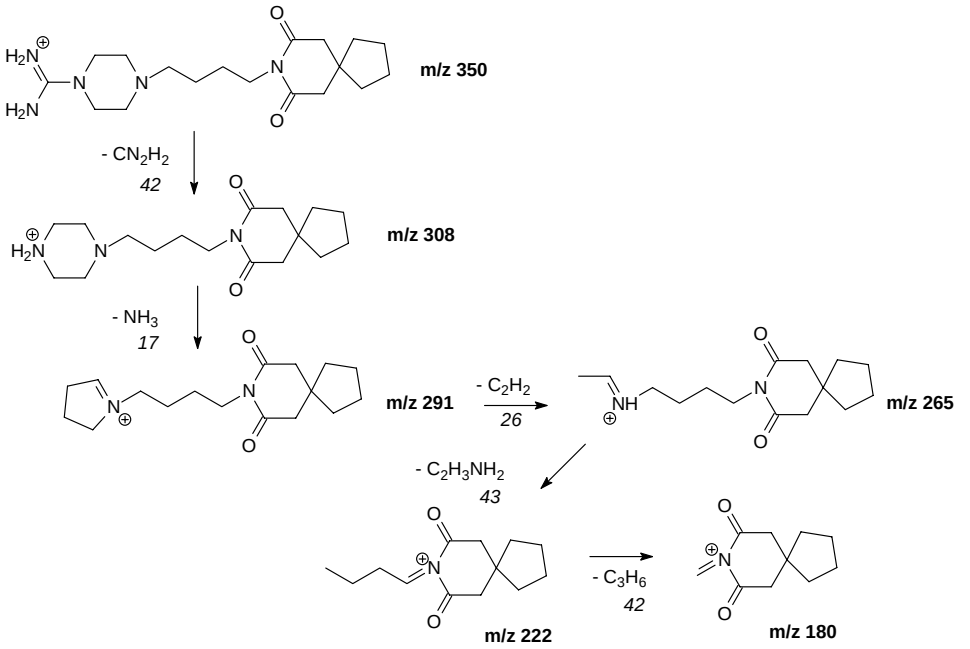

Scheme 6. Fragmentation followed by $[M + H]^+$ 350.

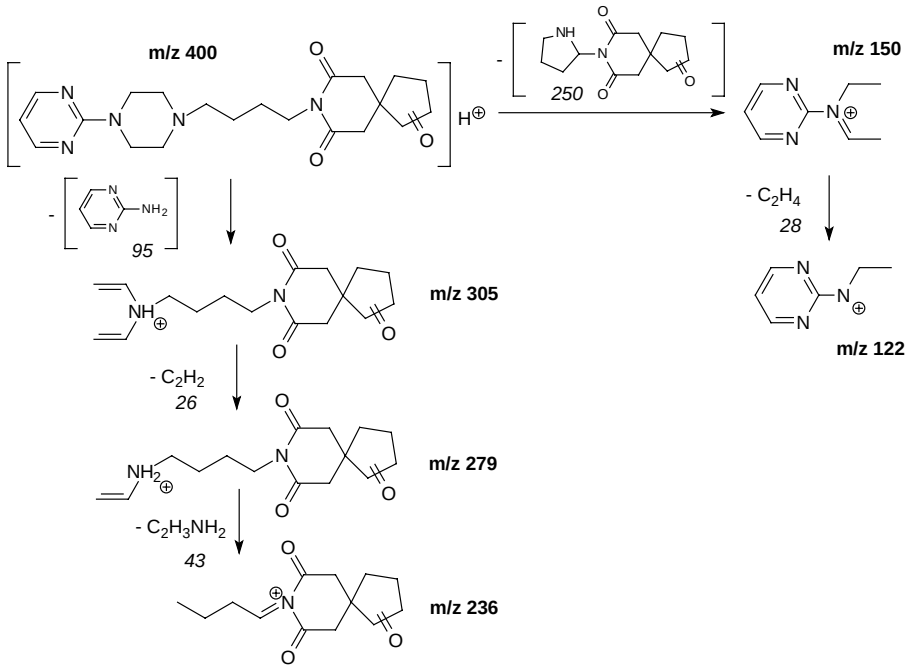

Scheme 7. Fragmentation of the structure at $[M + H]^+$ 400.

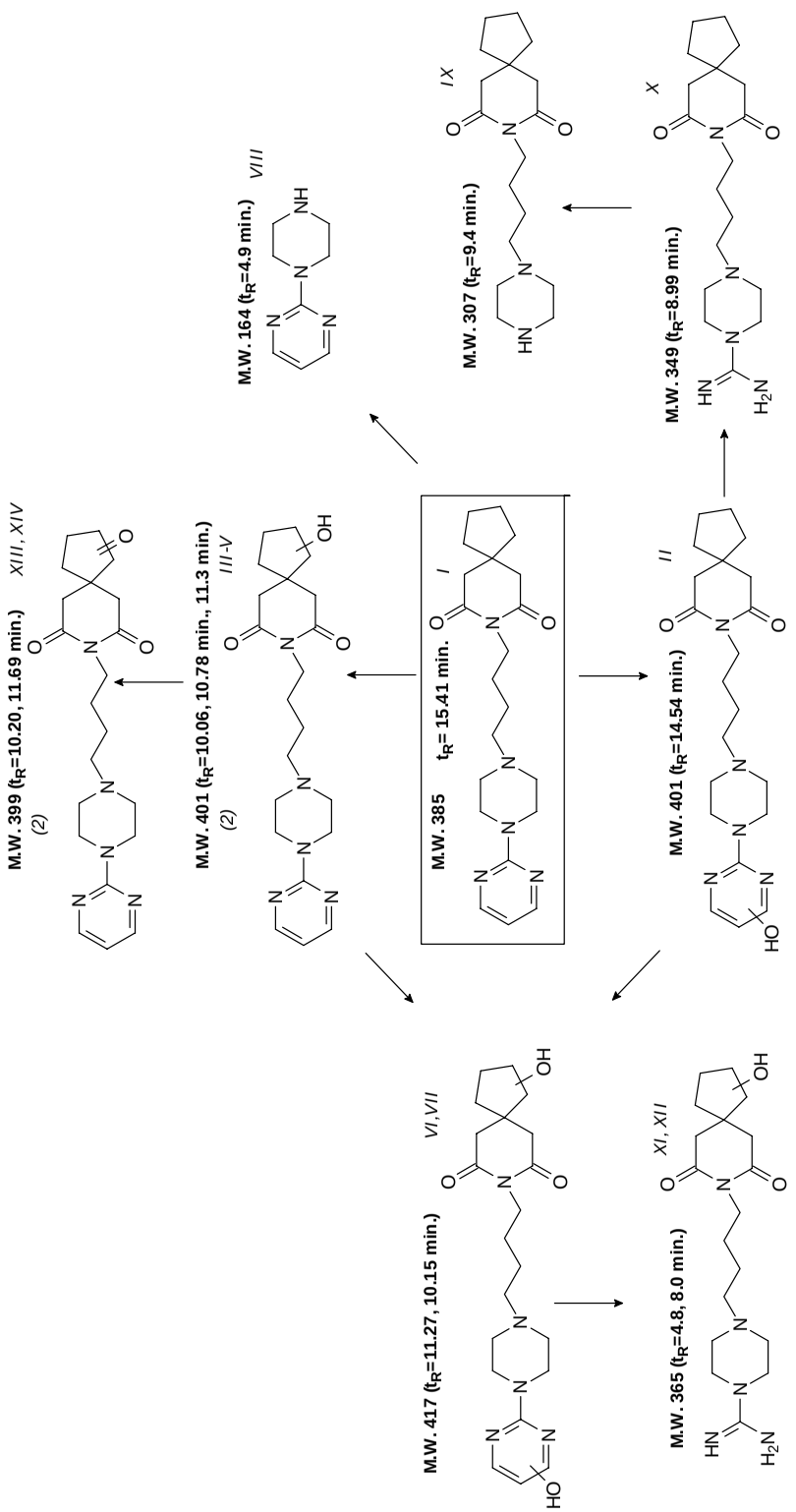

Scheme 8. Photocatalytic transformation pathways followed by buspirone.

the structure at $[M + H]^+$ 418 and they are attributed to the structures XI and XII in Table 1.

3.2.2.3. Structure with $[M + H]^+$ 400. The species holding $[M + H]^+$ 400 derives from the oxidation of the hydroxy-group present in the hydroxy-buspirone (Scheme 7).

As described above, the presence of the *m*/*z* 122 ion confirm the presence of unsubstituted pyrimidine substructure, while the shift of the *m*/*z* 307 to 305 ion, *m*/*z* 281 to 279 and *m*/*z* 238 to 236 evidences the oxidation of the hydroxyl group to the keto group. Two peaks holding the same *m*/*z* ratio have been identified. They correspond to the structures labeled XIII and XIV, coming from the oxidation of the OH group present in the structures III and IV (see Scheme 8).

4. Conclusions

More than one mechanism is involved into the photoinduced transformation process of buspirone. From the present study, several species have been identified and we have built a mechanism of transformation able to collect all the observed species. Hydroxylation occurs both on the pyrimidine substructure and on azaspirone decane dione substructure, so leading to several hydroxy and dihydroxy-buspirone structures. Moreover, the buspirone is degradated to form despyrimidinyl buspirone and 1-pyrimidinyl piperazine. Further oxidation occurs and leads to the transformation of the hydroxy-group into a keto group and to the breaking of the pyrimidine substructure.

Several of these structures have been also found into in vivo metabolic studies so that this methodology may be considered as a suitable tool to simulate in a laboratory experiment what occurs in living organism and to suggest new structures in yet to come metabolism studies.

References

[1] P. Calza, E. Pelizzetti, M. Brussino, C. Baiocchi, J. Am. Soc. Mass Spectrom. 12 (2001) 1286–1295.
[2] D.L. Temple, J.P. Yevich, J.S. New, J. Clin. Psychiatry 43 (1982) 4–9.
[3] J. Haller, J. Halasz, G.B. Makara, Behav. Pharmacol. 11 (2000) 403–412.
[4] M.Y. Dobson, R.D.E. Sewell, P.S.J. Spencer, J. Pharm. Pharmacol. 46 (1994) 1090–1095.
[5] L.K. Goa, A. Ward, Drugs 32 (1986) 114–129.
[6] M. Hascoet, M. Bourin, B.A.N. Dhonnchadha, Pharmacol. Biochem. Behav. 67 (2000) 45–53.
[7] M.E. Trulson, K. Arasteh, J. Pharm. Pharmacol. 38 (1986) 380–382.
[8] R.E. Gammans, E.H. Kerns, W.W. Bullen, J. Chromatogr. 345 (1985) 285–297.
[9] H. Jajoo, R. Mayol, J. LaBudde, I. Blair, Drug Metab. Dispos. 17 (1989) 634–640.
[10] H.K. Jajoo, I.A. Blair, L.J. Klunk, R.F. Mayol, Xenobiotica 8 (1990) 779–786.
[11] E.H. Kerns, R.A. Rourick, K.J. Volk, M.S. Lee, J. Chromatogr. B 698 (1997) 133–145.
[12] S.M.R. Stanley, J. Mass Spectrom. 35 (2000) 402–407.
[13] P. Betto, A. Meneguz, G. Ricciarello, S. Pichini, J. Chromatogr. 575 (1992) 117–121.
[14] M. Kartal, A. Khedr, A. Sakr, J. Chromatogr. Sci. 38 (2000) 151–156.
[15] F. Kristjànsson, J. Chromatogr. 566 (1991) 250–256.
[16] M. Franklin, J. Chromatogr. 526 (1990) 590–596.
[17] C. Minero, F. Catozzo, E. Pelizzetti, Langmuir 8 (1992) 481–486.
[18] M.A. Fox, M.T. Dulay, Chem. Rev. 93 (1993) 341–357.
[19] M.R. Hoffmann, S.T. Martin, W. Choi, D.W. Bahnemann, Chem. Rev. 95 (1995) 69–96.
[20] C. Minero, G. Mariella, V. Maurino, E. Pelizzetti, Langmuir 16 (2000) 2632–2641.
[21] D. Lawless, N. Serpone, D. Meisel, J. Phys. Chem. 95 (1991) 5166–5170.
[22] C.S. Turchi, D.F. Ollis, J. Catal. 119 (1989) 483–496.
[23] G.K.C. Low, G.R. McEvoy, R.W. Matthews, Environ. Sci. Technol. 25 (1991) 460–467.
[24] D.W. Bahnemann, J. Cunningham, M.A. Fox, E. Pelizzetti, P. Pichat, N. Serpone, in: G.R. Helz, R.G. Zepp, D.G. Crosby, Aquatic and Surface Chemistry, Lewis, Boca Raton, 1994, pp. 275–278.